Journal of Engineering Physics and Thermophysics, Vol. 73, No. 6, 2000

HOMOGENEITY OF THE ELECTRIC-DISCHARGE PLASMA IN A COAXIAL FLASH LAMP

B. A. Barikhin[*)] **and Yu. I. Kryshalovich**

UDC 533.9.082.715+681.7.069.24

The main factor that sharply decreases the efficiency of the employment of a pulsed-discharge xenon plasma as an emitter in electric-discharge sources of pumping of dye lasers is a macroscopic loss of stability of the discharge in the temperature and pressure ranges selected. It has been established that in the pressure range of 1–10 torr, an increase in the temperature of a pulsed-discharge xenon plasma results in the mechanism of conduction becoming purely collisional. Stabilization of macroinstabilities in the plasma has been attained using a sectioned return current conductor in a flash coaxial lamp. It has been verified by experiment that uniformity of the sectioning ensures a high degree of homogeneity of the electric-discharge plasma in the discharge space.

A current flow in an electric-discharge plasma is always associated to some extent with local disturbances of its quasineutrality and deviations from equilibrium. Here different kinds of wave motion, which in the equilibrium state are at the level of thermal fluctuations, can be initiated in the plasma. In particular, in the region of the velocity spectrum within which an ordered charge transfer is performed, the distribution of the electrons by velocities can markedly differ from a Maxwell distribution. In the case where the velocity of the ordered motion v_e differs from the most probable velocity of the thermal motion v_t, on the equilibrium-distribution profile there arises a second maximum near $\bar{v}_e$. The larger the difference between $\bar{v}_e$ and v_t, the more pronounced this maximum (even for a low density of the discharge current) [1]. It was experimentally established for xenon [2] that in the range of brightness temperatures $10^4 \le T_{pl} \le 3\cdot10^4$ K the strength of the external electric field in the interelectrode space varies, within the limits $0.2\cdot10^5 \le E_{ie} \le 1.8\cdot10^5$ V/m, with the square of the temperature of an equivalent source of equilibrium radiation T_{pl}^{eq} for which the most probable value of the velocity v_e^{eq} is approximately equal to $\bar{v}_e$. Consequently, $(\bar{v}_e/\bar{v}_t)^2 \approx T_{pl}^{eq}/T_{pl}$ and, in accordance with the data of Table 1, at $T_{pl} \approx 1.4\cdot10^4$ K in the range of xenon pressures $1.0 \le P_{Xe} \le 10$ torr this ratio decreases to $10^{-2} \ge (\bar{v}_e/v_t)^2 \ge 10^{-4}$. Because of this, at the low-temperature boundary of the temperature range, particles with velocities $\bar{v}_e \sim v_t$ are practically absent and hence electron energy cannot be transferred by plasma oscillations, which in this case, too, are not higher than the thermal background. As the temperature increases to $3\cdot10^4$ K in the above-mentioned pressure range, the velocity ratio increases significantly, $1 \ge (\bar{v}_e/v_t)^2 \ge 10^{-2}$. In this situation, the number of electrons moving with a velocity $\bar{v}_e \sim v_t$ is fairly large and energy should be transferred from the electronic component to a wave whose phase velocity differs insignificantly from v_t. This can build up plasma oscillations. Here the damping of oscillations with a wavelength longer than the Debye radius will be weak, which can lead to the appearance of instability.

It was established in [3] that the average brightness temperature of an electric-discharge plasma over the pulse is approximately half the temperature attained at the maximum of the pumping pulse. Because of this, for example, in a laser based on an alcoholic solution of rhodamine 6G, for which the optimum value of the brightness temperature of the pumping source is $\approx 1.3\cdot10^4$ K [3], even at the leading edge of the excitation pulse, beginning with $c \approx 2\cdot10^4$ K (Table 1), the electric-discharge plasma can become unstable. Since the brightness temperature continues to increase after the appearance of the instability, the latter can develop up to

*) Deceased.

Ya. Kupala Grodno State University, Grodno, Belarus. Translated from Inzhenerno-Fizicheskii Zhurnal, Vol. 73, No. 6, pp. 1234-1244, November–December, 2000. Original article submitted December 15, 1999.

1062-0125/00/7306-1195$25.00

TABLE 1. Ratio of the Energy of the Directed Motion of Electrons in a Discharge to the Energy of Their Thermal Motion

P_{Xe}, torr	n_{Xe}, m^{-3}	T_{pl}, K										
		10^4	$1.2\cdot10^4$	$1.4\cdot10^4$	$1.6\cdot10^4$	$1.8\cdot10^4$	$2.0\cdot10^4$	$2.2\cdot10^4$	$2.4\cdot10^4$	$2.6\cdot10^4$	$2.8\cdot10^4$	$3.0\cdot10^4$
		E_{ie}, V/m										
		$2\cdot10^4$	$2.88\cdot10^4$	$3.92\cdot10^4$	$5.12\cdot10^4$	$6.48\cdot10^4$	$8.0\cdot10^4$	$9.68\cdot10^4$	$10.52\cdot10^4$	$13.52\cdot10^4$	$15.68\cdot10^4$	$18.0\cdot10^4$
		Mean thermal velocity v_t, m/sec										
		$5.504\cdot10^5$	$6.029\cdot10^5$	$6.512\cdot10^5$	$6.962\cdot10^5$	$7.384\cdot10^5$	$7.784\cdot10^5$	$8.164\cdot10^5$	$8.527\cdot10^5$	$8.875\cdot10^5$	$9.210\cdot10^5$	$9.533\cdot10^5$
1.0	$0.0355\cdot10^{24}$	$1.401\cdot10^{-3}$	$4.184\cdot10^{-3}$	$1.055\cdot10^{-2}$	$2.318\cdot10^{-2}$	$4.754\cdot10^{-2}$	$8.960\cdot10^{-2}$	0.158	0.266	0.432	0.674	1.018
5.0	$0.1775\cdot10^{24}$	$5.549\cdot10^{-5}$	$1.674\cdot10^{-4}$	$4.171\cdot10^{-4}$	$9.360\cdot10^{-4}$	$1.902\cdot10^{-3}$	$3.584\cdot10^{-3}$	$6.339\cdot10^{-3}$	$1.067\cdot10^{-2}$	$1.708\cdot10^{-2}$	$2.688\cdot10^{-2}$	$4.099\cdot10^{-2}$
10.0	$0.355\cdot10^{24}$	$1.320\cdot10^{-5}$	$4.185\cdot10^{-5}$	$1.058\cdot10^{-4}$	$2.318\cdot10^{-4}$	$4.754\cdot10^{-4}$	$8.960\cdot10^{-4}$	$1.585\cdot10^{-3}$	$2.662\cdot10^{-3}$	$4.315\cdot10^{-3}$	$6.738\cdot10^{-3}$	$1.018\cdot10^{-2}$
15.0	$0.5325\cdot10^{24}$	$3.994\cdot10^{-6}$	$1.860\cdot10^{-5}$	$4.565\cdot10^{-5}$	$1.040\cdot10^{-4}$	$2.100\cdot10^{-4}$	$3.965\cdot10^{-4}$	$7.065\cdot10^{-4}$	$1.189\cdot10^{-3}$	$1.911\cdot10^{-3}$	$2.983\cdot10^{-3}$	$4.521\cdot10^{-3}$
20.0	$0.710\cdot10^{24}$	$3.301\cdot10^{-6}$	$9.932\cdot10^{-6}$	$2.568\cdot10^{-5}$	$5.795\cdot10^{-5}$	$1.174\cdot10^{-4}$	$2.221\cdot10^{-4}$	$3.938\cdot10^{-4}$	$6.657\cdot10^{-4}$	$1.075\cdot10^{-3}$	$1.684\cdot10^{-3}$	$2.546\cdot10^{-3}$
25.0	$0.8875\cdot10^{24}$	$2.220\cdot10^{-6}$	$7.043\cdot10^{-6}$	$1.719\cdot10^{-5}$	$3.639\cdot10^{-5}$	$7.512\cdot10^{-5}$	$1.427\cdot10^{-4}$	$2.536\cdot10^{-4}$	$4.260\cdot10^{-4}$	$6.892\cdot10^{-4}$	$1.075\cdot10^{-3}$	$1.631\cdot10^{-3}$
30.0	$1.065\cdot10^{24}$	$1.526\cdot10^{-6}$	$4.649\cdot10^{-6}$	$1.141\cdot10^{-5}$	$2.527\cdot10^{-5}$	$5.348\cdot10^{-5}$	$1.004\cdot10^{-4}$	$1.750\cdot10^{-4}$	$2.972\cdot10^{-4}$	$4.778\cdot10^{-4}$	$7.486\cdot10^{-4}$	$1.134\cdot10^{-3}$
35.0	$1.242\cdot10^{24}$	$1.149\cdot10^{-6}$	$3.329\cdot10^{-6}$	$8.513\cdot10^{-6}$	$1.857\cdot10^{-5}$	$3.881\cdot10^{-5}$	$7.189\cdot10^{-5}$	$1.298\cdot10^{-4}$	$2.183\cdot10^{-4}$	$3.498\cdot10^{-4}$	$5.501\cdot10^{-4}$	$8.332\cdot10^{-4}$
40.0	$1.420\cdot10^{24}$	$8.586\cdot10^{-7}$	$2.588\cdot10^{-6}$	$6.815\cdot10^{-6}$	$1.504\cdot10^{-5}$	$2.934\cdot10^{-5}$	$5.552\cdot10^{-5}$	$9.843\cdot10^{-5}$	$1.664\cdot10^{-4}$	$2.743\cdot10^{-4}$	$4.211\cdot10^{-4}$	$6.338\cdot10^{-4}$
50.0	$1.775\cdot10^{24}$	$5.549\cdot10^{-7}$	$1.674\cdot10^{-6}$	$3.985\cdot10^{-6}$	$9.098\cdot10^{-6}$	$1.878\cdot10^{-5}$	$3.492\cdot10^{-5}$	$6.339\cdot10^{-5}$	$1.065\cdot10^{-4}$	$1.708\cdot10^{-4}$	$2.688\cdot10^{-4}$	$4.056\cdot10^{-4}$
100.0	$3.550\cdot10^{24}$	$1.320\cdot10^{-7}$	$4.184\cdot10^{-7}$	$1.058\cdot10^{-6}$	$2.496\cdot10^{-6}$	$4.695\cdot10^{-6}$	$8.731\cdot10^{-6}$	$1.536\cdot10^{-5}$	$2.662\cdot10^{-5}$	$4.271\cdot10^{-5}$	$6.809\cdot10^{-5}$	$1.014\cdot10^{-4}$

a jump-like change to another state and disintegrate. In particular, for the above-mentioned pressure an increase in the temperature of the pulsed-discharge xenon plasma leads to a change in its conduction [2] because of the change from the mechanism of compensation for collisional conduction by conduction that is due to the Ramsauer effect to a purely collisional mechanism. As the conduction of the plasma increases, the release of Joule heat in its bulk increases proportionally to E_{ie}^2, since $j_{ie}^2/\sigma_e = \sigma_e E_{ie}^2$; but, this results in an increase in the rate of the temperature rise, i.e., in the plasma a distinctive thermal instability arises. In this simplified consideration, any equilibrium in which the conduction σ_e and hence the temperature T_{pl} of the plasma and its density (in the case where the plasma is not fully ionized) change in space should be unstable. In this case, the model can be refined first of all by taking account of the equalizing action of heat conduction, for example, along the magnetic-field lines. Thus, besides the development of the instability representing an oscillation process with an amplitude increasing with time, there is the possibility of an "aperiodic" development that gives rise to a deviation from the initial state that increases monotonically with time [4].

The type of instability of the pulsed-discharge plasma in xenon at a pressure $1.0 \le P_{Xe} \le 10$ torr with a brightness temperature $10^4 \le T_{pl} \le 3\cdot10^4$K is predominantly determined by the character of its imperfection, which is described by three similarity numbers [4] – the hydrodynamic Reynolds number $Re_g = \tau_g/\tau$, magnetic Reynolds number $Re_m = \tau_m/\tau$, and Peclet number $Pe = \tau_t/\tau$. These ratios involve the time scale $\tau = L_{ie}/\bar{v}_e$, which was $0.5 \le \tau \le 10^2$ μsec in the experiments [3], the characteristic time of the "hydrodynamic diffusion" $\tau_g = L_{ie}^2/\nu$, the characteristic time of the "magnetic diffusion" $\tau_m = L_{ie}^2/\xi_m$, and the characteristic time of the "convective diffusion" $\tau_t = L_{ie}^2/\chi_t$, where $L_{ie} \approx 0.5$ m is the length of the interelectrode space of the coaxial flash lamp [3]; ν is the kinematic viscosity of the plasma, estimated in [3] as $\nu \sim 10^{-5}$ m^2/sec; χ_t is the thermal diffusivity of the plasma, estimated in [3] as $\chi_t \sim 0.1$ m^2/sec; $\bar{v}_e = eE_{ie}\tau_{ei}/m_e$ is the mean velocity of the directed motion of electrons, whose values measured in [3] are given in Table 2; $\xi_m = \varepsilon_0 c^2/\sigma_e$ is the magnetic viscosity of the plasma, expressed in terms of its conduction σ_e. The values of ξ_m calculated from the experimental data of [3] are given in Table 3 and the corresponding values of the magnetic Reynolds number are given in Table 4. For the brightness temperature of the plasma $T_{pl} \approx 1.4\cdot10^4$ K in the investigated range of xenon pressures, $\bar{v}_e \sim 10^4$ m/sec and $\xi_m \approx 10^2$ m^2/sec.

Thus, at $Re_g >> 1$, $Pe >> 1$, and $Re_m \approx 50$ the slight disruption of the plasma perfection can be due to the increased magnetic viscosity, which enhances the dissipation of the magnetic field energy, i.e., the "unsticking" of the plasma from the field lines. This disruption is not related to the pinching of the entire plasma cylinder in the range $5 \le P_{Xe} \le 10$ torr, as follows from the results given in Table 5; however, at $P_{Xe} \approx 1$ torr the Bennet criterion is already fulfilled for the entire volume of the plasma. Consequently, the probability of local pinching in this region, even at the expense of fluctuations that are due to the "unsticking," is significantly increased, i.e., discharge contraction can occur.

Because of this, the main factor sharply decreasing the efficiency of the employment of a pulsed-discharge xenon plasma as an emitter in electric-discharge sources of pumping of dye lasers [2, 5] is macroscopic loss of stability of the discharge in the temperature and pressure ranges selected. If there is no macroscopic stabilization of the discharge, any attempts to suppress the microinstability in the discharge plasma lose their meaning. The coaxial design of the pumping source usually requires [5, 6] the use of a coaxial solid return current conductor and a coaxial cylindrical plasma layer. The magnetic-field fluctuations are predominantly due to the Taylor instability of the discharge current flow in the metal surface layer of the return current conductor. The stability of the flow is usually determined [4] by the critical value T_{cr} of the Taylor number

$$T \sim \left(\frac{\Delta R_{d.sp}}{\lambda_{d.sp}}\right)^4 \left[1 + H^2 \left(\frac{\lambda_{d.sp}}{\Delta R_{d.sp}}\right)^2\right] \qquad (1)$$

(for a rigid cylindrical surface $T_{cr} \approx 1700$), where $\Delta R_{d.sp}$ is the thickness of the clearance between the coaxial cylinders; $\lambda_{d.sp}$ is the mean magnitude of the disturbance;

TABLE 2. Mean Velocity of Electron Flow

P_{Xe}, torr	n_{Xe}, m^{-3}	T_{pl}, K										
		10^4	$1.2 \cdot 10^4$	$1.4 \cdot 10^4$	$1.6 \cdot 10^4$	$1.8 \cdot 10^4$	$2.0 \cdot 10^4$	$2.2 \cdot 10^4$	$2.4 \cdot 10^4$	$2.6 \cdot 10^4$	$2.8 \cdot 10^4$	$3.0 \cdot 10^4$
		U_0, V										
		10^4	$1.44 \cdot 10^4$	$1.96 \cdot 10^4$	$2.56 \cdot 10^4$	$3.24 \cdot 10^4$	$4.0 \cdot 10^4$	$4.84 \cdot 10^4$	$5.76 \cdot 10^4$	$6.76 \cdot 10^4$	$7.84 \cdot 10^4$	$9.0 \cdot 10^4$
		E_{ie}, V/m										
		$2 \cdot 10^4$	$2.88 \cdot 10^4$	$3.92 \cdot 10^4$	$5.12 \cdot 10^4$	$6.48 \cdot 10^4$	$8.0 \cdot 10^4$	$9.68 \cdot 10^4$	$10.52 \cdot 10^4$	$13.52 \cdot 10^4$	$15.68 \cdot 10^4$	$18.0 \cdot 10^4$
1.0	$0.0355 \cdot 10^{24}$	$2.06 \cdot 10^4$	$3.90 \cdot 10^4$	$6.69 \cdot 10^4$	$1.06 \cdot 10^4$	$16.1 \cdot 10^4$	$23.3 \cdot 10^4$	$32.5 \cdot 10^4$	$44.0 \cdot 10^4$	$58.3 \cdot 10^4$	$75.6 \cdot 10^4$	$96.2 \cdot 10^4$
5.0	$0.1775 \cdot 10^{24}$	$0.41 \cdot 10^4$	$0.78 \cdot 10^4$	$1.33 \cdot 10^4$	$2.13 \cdot 10^4$	$3.22 \cdot 10^4$	$4.66 \cdot 10^4$	$6.50 \cdot 10^4$	$8.81 \cdot 10^4$	$11.6 \cdot 10^4$	$15.1 \cdot 10^4$	$19.3 \cdot 10^4$
10.0	$0.355 \cdot 10^{24}$	$0.20 \cdot 10^4$	$0.39 \cdot 10^4$	$0.67 \cdot 10^4$	$1.06 \cdot 10^4$	$1.61 \cdot 10^4$	$2.33 \cdot 10^4$	$3.25 \cdot 10^4$	$4.40 \cdot 10^4$	$5.83 \cdot 10^4$	$7.56 \cdot 10^4$	$9.62 \cdot 10^4$
15.0	$0.5325 \cdot 10^{24}$	$0.11 \cdot 10^4$	$0.26 \cdot 10^4$	$0.44 \cdot 10^4$	$0.71 \cdot 10^4$	$1.07 \cdot 10^4$	$1.55 \cdot 10^4$	$2.17 \cdot 10^4$	$2.94 \cdot 10^4$	$3.88 \cdot 10^4$	$5.03 \cdot 10^4$	$6.41 \cdot 10^4$
20.0	$0.710 \cdot 10^{24}$	$0.10 \cdot 10^4$	$0.19 \cdot 10^4$	$0.33 \cdot 10^4$	$0.53 \cdot 10^4$	$0.80 \cdot 10^4$	$1.16 \cdot 10^4$	$1.62 \cdot 10^4$	$2.20 \cdot 10^4$	$2.91 \cdot 10^4$	$3.78 \cdot 10^4$	$4.81 \cdot 10^4$
25.0	$0.8875 \cdot 10^{24}$	$0.082 \cdot 10^4$	$0.16 \cdot 10^4$	$0.27 \cdot 10^4$	$0.42 \cdot 10^4$	$0.64 \cdot 10^4$	$0.93 \cdot 10^4$	$1.30 \cdot 10^4$	$1.76 \cdot 10^4$	$2.33 \cdot 10^4$	$3.02 \cdot 10^4$	$3.85 \cdot 10^4$
30.0	$1.065 \cdot 10^{24}$	$0.068 \cdot 10^4$	$0.13 \cdot 10^4$	$0.22 \cdot 10^4$	$0.35 \cdot 10^4$	$0.54 \cdot 10^4$	$0.78 \cdot 10^4$	$1.08 \cdot 10^4$	$1.47 \cdot 10^4$	$1.94 \cdot 10^4$	$2.52 \cdot 10^4$	$3.21 \cdot 10^4$
35.0	$1.242 \cdot 10^{24}$	$0.059 \cdot 10^4$	$0.11 \cdot 10^4$	$0.19 \cdot 10^4$	$0.30 \cdot 10^4$	$0.46 \cdot 10^4$	$0.66 \cdot 10^4$	$0.93 \cdot 10^4$	$1.26 \cdot 10^4$	$1.66 \cdot 10^4$	$2.16 \cdot 10^4$	$2.75 \cdot 10^4$
40.0	$1.420 \cdot 10^{24}$	$0.051 \cdot 10^4$	$0.097 \cdot 10^4$	$0.17 \cdot 10^4$	$0.27 \cdot 10^4$	$0.40 \cdot 10^4$	$0.58 \cdot 10^4$	$0.81 \cdot 10^4$	$1.10 \cdot 10^4$	$1.47 \cdot 10^4$	$1.89 \cdot 10^4$	$2.40 \cdot 10^4$
50.0	$1.775 \cdot 10^{24}$	$0.041 \cdot 10^4$	$0.078 \cdot 10^4$	$0.13 \cdot 10^4$	$0.21 \cdot 10^4$	$0.32 \cdot 10^4$	$0.46 \cdot 10^4$	$0.65 \cdot 10^4$	$0.88 \cdot 10^4$	$1.16 \cdot 10^4$	$1.51 \cdot 10^4$	$1.92 \cdot 10^4$
100.0	$3.550 \cdot 10^{24}$	$0.020 \cdot 10^4$	$0.039 \cdot 10^4$	$0.067 \cdot 10^4$	$0.11 \cdot 10^4$	$0.16 \cdot 10^4$	$0.23 \cdot 10^4$	$0.32 \cdot 10^4$	$0.44 \cdot 10^4$	$0.58 \cdot 10^4$	$0.76 \cdot 10^4$	$0.96 \cdot 10^4$

TABLE 3. Magnetic Viscosity of the Electronic Component

P_{Xe}, torr	n_{Xe}, m^{-3}	T_{pl}, K										
		10^4	$1.2 \cdot 10^4$	$1.4 \cdot 10^4$	$1.6 \cdot 10^4$	$1.8 \cdot 10^4$	$2.0 \cdot 10^4$	$2.2 \cdot 10^4$	$2.4 \cdot 10^4$	$2.6 \cdot 10^4$	$2.8 \cdot 10^4$	$3.0 \cdot 10^4$
		U_0, V										
		10^4	$1.44 \cdot 10^4$	$1.96 \cdot 10^4$	$2.56 \cdot 10^4$	$3.24 \cdot 10^4$	$4.0 \cdot 10^4$	$4.84 \cdot 10^4$	$5.76 \cdot 10^4$	$6.76 \cdot 10^4$	$7.84 \cdot 10^4$	$9.0 \cdot 10^4$
		E_{ie}, V/m										
		$2 \cdot 10^4$	$2.88 \cdot 10^4$	$3.92 \cdot 10^4$	$5.12 \cdot 10^4$	$6.48 \cdot 10^4$	$8.0 \cdot 10^4$	$9.68 \cdot 10^4$	$10.52 \cdot 10^4$	$13.52 \cdot 10^4$	$15.68 \cdot 10^4$	$18.0 \cdot 10^4$
1.0	$0.0355 \cdot 10^{24}$	175.83	117.22	82.21	60.86	46.54	36.80	29.58	24.25	20.35	17.25	14.79
5.0	$0.1775 \cdot 10^{24}$	121.73	81.15	57.03	42.20	32.30	25.42	20.55	16.88	14.10	11.94	10.21
10.0	$0.355 \cdot 10^{24}$	74.47	49.45	34.78	25.94	19.84	15.63	12.61	10.36	8.67	7.31	6.25
15.0	$0.5325 \cdot 10^{24}$	48.69	32.30	22.93	16.88	12.94	10.78	9.35	8.20	7.28	6.50	5.87
20.0	$0.710 \cdot 10^{24}$	34.40	23.19	18.45	15.07	12.94	10.78	9.35	8.20	7.28	6.50	5.87
25.0	$0.8875 \cdot 10^{24}$	30.43	23.19	18.45	15.07	12.94	10.78	9.35	8.20	7.28	6.50	5.87
30.0	$1.065 \cdot 10^{24}$	30.43	23.19	18.45	15.07	12.94	10.78	9.35	8.20	7.28	6.50	5.87
35.0	$1.242 \cdot 10^{24}$	30.43	23.19	18.45	15.07	12.94	10.78	9.35	8.20	7.28	6.50	5.87
40.0	$1.420 \cdot 10^{24}$	30.43	23.19	18.45	15.07	12.94	10.78	9.35	8.20	7.28	6.50	5.87
50.0	$1.775 \cdot 10^{24}$	30.43	23.19	18.45	15.07	12.94	10.78	9.35	8.20	7.28	6.50	5.87
10.0	$3.550 \cdot 10^{24}$	30.43	23.19	18.45	15.07	12.94	10.78	9.35	8.20	7.28	6.50	5.87

TABLE 4. Magnetic Reynolds Number for the Electronic Component

P_{Xe}, torr	n_{Xe}, m $^{-3}$	T_{pl}, K										
		10^4	$1.2 \cdot 10^4$	$1.4 \cdot 10^4$	$1.6 \cdot 10^4$	$1.8 \cdot 10^4$	$2.0 \cdot 10^4$	$2.2 \cdot 10^4$	$2.4 \cdot 10^4$	$2.6 \cdot 10^4$	$2.8 \cdot 10^4$	$3.0 \cdot 10^4$
		E_{ie}, V/m										
		$2 \cdot 10^4$	$2.88 \cdot 10^4$	$3.92 \cdot 10^4$	$5.12 \cdot 10^4$	$6.48 \cdot 10^4$	$8.0 \cdot 10^4$	$9.68 \cdot 10^4$	$10.52 \cdot 10^4$	$13.52 \cdot 10^4$	$15.68 \cdot 10^4$	$18.0 \cdot 10^4$
1.0	$0.0355 \cdot 10^{24}$	58.58	166.35	406.88	870.85	$1.73 \cdot 10^3$	$3.16 \cdot 10^3$	$5.49 \cdot 10^3$	$9.07 \cdot 10^3$	$1.43 \cdot 10^4$	$2.19 \cdot 10^4$	$3.25 \cdot 10^4$
5.0	$0.1775 \cdot 10^{24}$	16.84	48.05	116.6	252.37	498.45	916.6	$1.58 \cdot 10^3$	$2.61 \cdot 10^3$	$4.11 \cdot 10^3$	$6.32 \cdot 10^3$	$9.45 \cdot 10^3$
10.0	$0.355 \cdot 10^{24}$	13.43	39.43	96.32	204.32	405.74	745.36	$1.29 \cdot 10^3$	$2.12 \cdot 10^3$	$3.36 \cdot 10^3$	$5.17 \cdot 10^3$	$7.70 \cdot 10^3$
15.0	$0.5325 \cdot 10^{24}$	11.31	40.24	95.94	210.30	413.45	718.92	$1.16 \cdot 10^3$	$1.79 \cdot 10^3$	$2.66 \cdot 10^3$	$3.87 \cdot 10^3$	$5.46 \cdot 10^3$
20.0	$0.710 \cdot 10^{24}$	14.53	40.96	89.43	175.85	309.12	538.03	866.31	$1.34 \cdot 10^3$	$2.00 \cdot 10^3$	$2.91 \cdot 10^3$	$4.10 \cdot 10^3$
25.0	$0.8875 \cdot 10^{24}$	13.47	34.50	73.17	139.35	247.30	431.35	695.19	$1.07 \cdot 10^3$	$1.6 \cdot 10^3$	$2.32 \cdot 10^3$	$3.28 \cdot 10^3$
30.0	$1.065 \cdot 10^{24}$	11.17	28.03	59.62	116.12	208.65	361.78	577.54	896.34	$1.33 \cdot 10^3$	$1.94 \cdot 10^3$	$2.73 \cdot 10^4$
35.0	$1.242 \cdot 10^{24}$	9.70	23.72	51.49	99.54	177.74	306.12	497.33	768.29	$1.14 \cdot 10^3$	$1.66 \cdot 10^3$	$2.34 \cdot 10^3$
40.0	$1.420 \cdot 10^{24}$	8.38	20.91	46.07	89.58	154.56	269.02	433.16	670.73	$1.01 \cdot 10^3$	$1.45 \cdot 10^3$	$2.04 \cdot 10^3$
50.0	$1.775 \cdot 10^{24}$	6.74	16.82	35.23	69.67	123.65	213.36	347.59	536.58	796.70	$1.16 \cdot 10^3$	$1.64 \cdot 10^3$
100.0	$3.550 \cdot 10^{24}$	3.29	8.41	18.61	36.50	61.82	106.68	171.12	268.29	398.35	584.62	817.72

TABLE 5. Threshold of Plasma Pinching $\beta_m \approx 0.588t^3/N_e$

P_{Xe}, torr	n_{Xe}, m^{-3}	T, K										
		10^4	$1.2 \cdot 10^4$	$1.4 \cdot 10^4$	$1.6 \cdot 10^4$	$1.8 \cdot 10^4$	$2.0 \cdot 10^4$	$2.2 \cdot 10^4$	$2.4 \cdot 10^4$	$2.6 \cdot 10^4$	$2.8 \cdot 10^4$	$3.0 \cdot 10^4$
		U_0, V										
		10^4	$2.88 \cdot 10^4$	$3.92 \cdot 10^4$	$5.12 \cdot 10^4$	$6.48 \cdot 10^4$	$8.0 \cdot 10^4$	$9.68 \cdot 10^4$	$10.52 \cdot 10^4$	$13.52 \cdot 10^4$	$15.68 \cdot 10^4$	$18.0 \cdot 10^4$
		I_{max}, A										
		$2 \cdot 10^5$	$2.88 \cdot 10^5$	$3.92 \cdot 10^5$	$5.12 \cdot 10^5$	$6.48 \cdot 10^5$	$8.0 \cdot 10^5$	$9.68 \cdot 10^5$	$11.52 \cdot 10^5$	$13.52 \cdot 10^5$	$15.68 \cdot 10^5$	$18.0 \cdot 10^5$
1.0	$0.0355 \cdot 10^{24}$	94.839	143.098	201.625	273.636	357.083	452.308	559.018	677.33	813.780	963.284	1125.957
5.0	$0.1775 \cdot 10^{24}$	13.154	19.882	28.052	37.921	49.395	62.470	77.488	94.183	112.828	133.485	155.647
10.0	$0.355 \cdot 10^{24}$	4.030	6.084	8.580	11.633	15.168	19.200	23.806	30.905	34.681	40.848	47.676
15.0	$0.5325 \cdot 10^{24}$	1.760	2.653	3.769	5.059	6.592	8.834	11.758	15.264	19.408	24.240	29.814
20.0	$0.710 \cdot 10^{24}$	0.935	1.431	2.272	3.392	4.828	6.625	8.818	11.448	14.556	18.180	22.360
25.0	$0.8875 \cdot 10^{24}$	0.662	1.145	1.817	2.713	3.862	5.300	7.055	9.158	11.645	14.544	17.888
30.0	$1.065 \cdot 10^{24}$	0.552	0.954	1.514	2.261	3.219	4.417	5.879	7.632	9.704	12.120	14.907
35.0	$1.242 \cdot 10^{24}$	0.473	0.818	1.229	1.939	2.760	3.548	5.879	6.544	8.321	10.393	12.783
40.0	$1.420 \cdot 10^{24}$	0.414	0.715	1.136	1.696	2.414	3.313	5.041	5.724	7.278	9.090	11.180
50.0	$1.775 \cdot 10^{24}$	0.331	0.572	0.909	1.357	1.931	2.650	4.409	4.579	5.822	7.272	8.944
100.0	$3.550 \cdot 10^{24}$	0.166	0.286	0.454	0.678	0.966	1.325	3.527	2.290	2.911	3.636	4.472

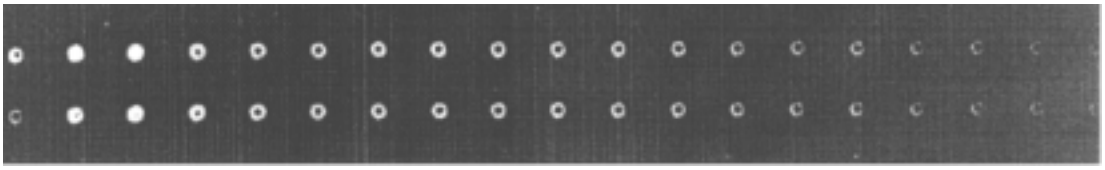

Fig. 1. Chronogram of the distribution of the radiation intensity along the perimeter of the cross section of the discharge space of a lamp. The time interval between the frames is 0.5 μsec.

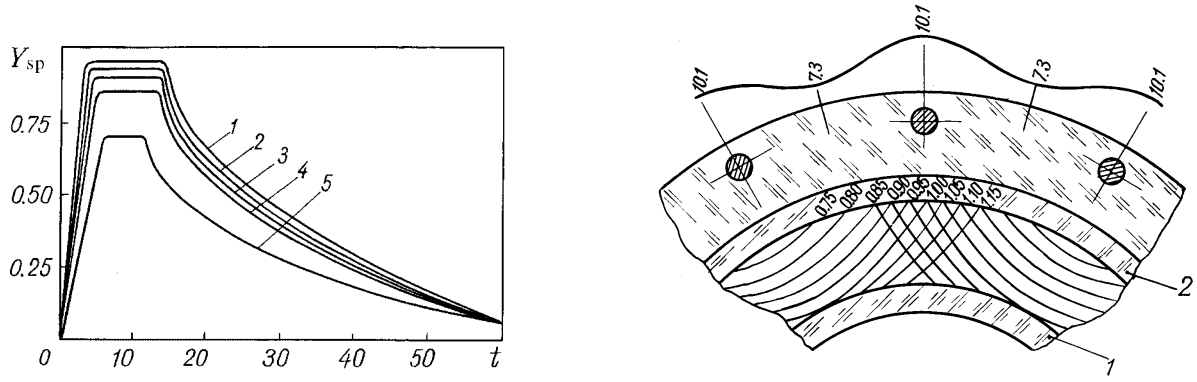

Fig. 2. Time dependence of the coefficient of filling of the cross section of the discharge space with the plasma for different values of the voltage across the capacitor bank: 1) 18 kV; 2) 15; 3) 12; 4) 9; 5) 6. Y_{sp}, %; t, μsec.

Fig. 3. Relative distribution of the magnetic pressure in the cross section of the discharge space of a lamp: 1, 2) inner and outer quartz pipes. The distance between the force lines and the relative magnetic pressure are dimensionless quantities.

$$H^2 = \mu_0 \frac{\sigma_{\tilde{n}} H_{d.sp}^2}{\zeta_{\tilde{n}}} (\Delta R_{d.sp})^2 \qquad (2)$$

is the Hartmann number squared, which depends on the conduction of the current-conductor material σ_c, the strength of the magnetic field in the clearance $H_{d.sp}$, and the dynamic viscosity of the electron gas in the metal [7]

$$\zeta_c = 0.4\tau_{\tilde{a}} n_{\tilde{a}} \varepsilon_F . \qquad (3)$$

Here $n_e \approx 8.47 \cdot 10^{28}$ m^{-3}, $\tau_e \approx 2.7 \cdot 10^{-14}$ sec, and $\varepsilon_F \approx 1.12 \cdot 10^{-18}$ J [8]; consequently, $\zeta_c \approx 10^{-3}$ Pa·sec and $H^2 \sim 10^7$. Even if the mean magnitude of the disturbance is $\lambda_{d.sp} \sim \Delta R_{d.sp}$, then $T/T_{cr} \sim 10^4 >> 1$ and the boundary of the current-flow stability in the return current conductor is significantly exceeded, and the disruption of the stability is macroscopic in character.

Stabilization of steady-state finite disturbances in an electric field is most effectively performed by means of their localization by increasing the depth of the potential well. In particular, this can be attained in the case where the return current conductor is made in the form of an aggregate of current-carrying pipes insulated from each other and positioned axially relative to the discharge space of the lamp. It is apparent that in this geometry, the density of the magnetic-field energy near the pipe is increased and it suppresses the development of azimuthal currents that appear in the basic conductor as a disturbance of the electric field between the electrodes. The stability of a current flow in a sectioned current conductor is regulated fairly automatically, since the density of the current in each pipe is significantly higher than the mean density of the current in the cross section of a solid cylinder having the same diameter. If the pipes are distributed uniformly

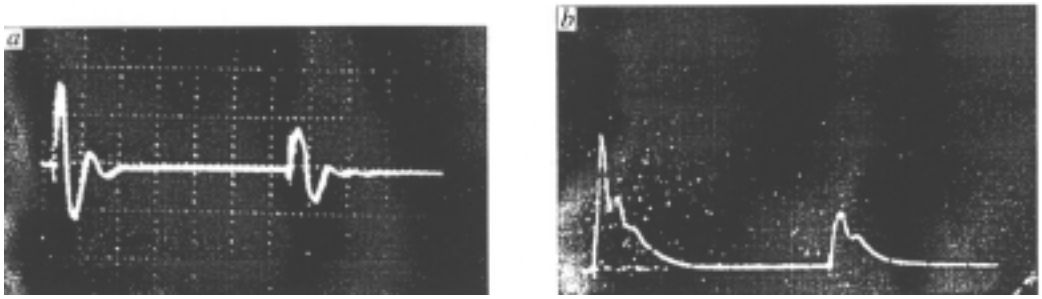

Fig. 4. Oscillograms of the discharge-current strength (a) and the optical pumping pulse (b) in the two-pulse regime at U_{cap} = 35 kV and t_d = 100 μsec; the time base is 20 μsec/div.

along the perimeter of the discharge space, the necessary degree of homogeneity of the electric-discharge plasma in the discharge space can be attained, which has been vierified by experiments [3, 9] in which stabilization of macroscopic disturbances was attained due to a technical design developed based on an analysis performed in the course of engineering work on the lamp. This is evidenced by chronograms of the distribution of the radiation intensity along the perimeter of the cross section of the discharge space of the lamp [3, 9], one of which with a time resolution of 0.5 μsec between the frames is shown in Fig. 1. Results of photometric measurement of the chronograms are given in Fig. 2, where the time dependence of the coefficient of uniformity of filling of the cross section of the discharge space with the plasma is shown for different values of the voltage across the capacitor bank of the power source. Figure 3 shows a qualitative picture of the distribution of the magnetic pressure in the cross section, calculated for a set of 12 current-carrying pipes, in relation to the pressure produced as a result of a current flow in a coaxial formed by two infinitely thin cylinders. The totality of all the experimental and calculation data points to stability of the current flow in the pulsed-discharge plasma of a lamp with a sectioned return current conductor.

A no less convincing proof of this is the similarity of the electrophysical and optical characteristics of the pulses in the case of commutation of two sections of the capacitive storage to the lamp [10]. Processing of the experimental data shows that in the regime of series connection of two pumping pulses with a delay between the pulses of up to ≈1 μsec the differences between the pulses are small, and they are not fundamental in nature: for the maximum current, the active resistance of the discharge plasma in the second pulse is ≈1.3 times that in the first pulse. In the experiments we used two sections of the storage with a capacity of 75 μF each with a controlled delay between pulses $10 \le t_d \le 10^3$ μsec; the level of the working voltage U_{cap} across each section could be selected independently. Figure 4a shows an oscillogram of the strength of the discharge current at U_{cap} = 35 kV and a delay between the pulses of 100 μsec, while Fig. 4b shows an oscillogram of an optical pumping pulse under the same conditions. The difference between the pulses became even smaller when the working voltage across the second section was somewhat higher than that across the first section. For example, for the experimental conditions (see Fig. 4) such a decrease was attained even at a working voltage across the second section of 40 kV.

Thus, a high degree of homogeneity of a discharge plasma makes it possible to obtain the maximum attainable energy of its radiation at the leading edge of the pumping pulse. By optimization of the discharge regime, up to 0.7 of the energy stored in the storage can be released in the active resistance [5]. In a regime with compensation for plasma conduction [2] achievedd by optimum selection of the brightness temperature and the working gas pressure, a large amount of luminous pumping energy can be obtained in the absorption band of the laser active medium, for example, for an alcoholic solution of rhodamine 6G, up to 0.25 of the total energy of the plasma radiation. Suppression of finite disturbances of the discharge current provides the minimum level of losses by excitation of instabilities in the discharge plasma. Moreover, a high degree of plasma homogeneity increases the uniformity of irradiation of the outer surface of the active medium by the pumping radiation in a cylindrical geometry.

NOTATION

T_{pl}, plasma temperature; T, Taylor number; T_{cr}, critical value of the Taylor number; P_{Xe}, xenon pressure; H, Hartmann number; U_{cap}, working voltage across the capacitor bank; E_{ie}, strength of the external electric field in the interelectrode space; σ_e, conduction of the electronic component of the plasma; j_{ie}, density of the current in the interelectrode space; n_e, density of electrons in the metal; τ_e, electronic relaxation time; ε_F, Fermi energy for copper; ε_0, dielectric constant; v_e, velocity of the directed motion of electrons; $\bar{v}_t$, mean velocity of the thermal motion of electrons; ζ_c, dynamic viscosity of the electron gas in the metal; c, velocity of light in vacuum; μ_0, permeability of vacuum; e, electron charge; n_{Xe}, xenon concentration; m_e, electron mass; β_m, threshold of plasma pinching; τ_{ei}, mean time between two collisions of an electron and an ion; N_e, number of electrons per cm of the plasma length; Y_{sp}, cross section of the discharge space; t, time. Subscripts and superscrips: max, maximum; eq, equivalent; e, electron; pl, plasma; t, thermal motion; ie, interelectrode; Xe, xenon; cr, critical; c, conductor; cap, capacitor; d, delay; m, magnetic; d.sp, discharge space; sp, space.

REFERENCES

1. L. A. Artsimovich and R. Z. Sagdeev, *Plasma Physics for Physicists* [in Russian], Moscow (1979).
2. B. A. Barikhin and Yu. I. Kryshalovich, *Inzh.-Fiz. Zh.*, **73**, No. 6, 1220-1228 (2000).
3. F. N. Baltakov and B. A. Barikhin, *Kvant. Élektronika*, **2**, No. 4, 822-826 (1975).
4. A. A. Vvedenov, E. P. Velikhov, and R. Z. Sagdeev, *Usp. Fiz. Nauk*, **73**, No. 4, 701-766 (1961).
5. E. F. Zholobov, D. I. Zenkov, A. I. Pavlovskii, et al., *Kvant. Elektronika*, **4**, No. 1, 122-128 (1977).
6. M. I. Dzyubenko, A. Ya. Matveev, and I. G. Naumenko, *Prib. Tekh. Éksp.*, No. 1, 171-173 (1972).
7. C. Kittel, *Quantum Theory of Solids* [Russian translation], Moscow (1967).
8. N. Ashcroft and N. Mermin, in: *Solid State Physics* [Russian translation], Moscow (1979), pp. 20, 24, and 51.
9. B. A. Barikhin, B. S. Makaev, L. V. Sukhanov, and A. I. Pavlovskii, *Kvant. Élektronika*, **3**, No. 6, 1211-1216 (1976).
10. B. A. Barikhin, A. Yu. Ivanov, E. V. Kudryavkin, and V. I. Nedolugov, *Kvant. Élektronika*, **21**, No. 4, 301-302 (1994).